

Automated Detection of Myocardial Infraction Disease from ECG Signal

Rohan Agarwal¹, Vaibhav Shresth¹, Veena Devi²

UG Student, Department of Electronics and Communication, RV College of Engineering, Bangalore, India¹

Associate Professor, Department of Electronics and Communication, RV College of Engineering, Bangalore, India²

ABSTRACT: The occlusion in one of the coronary arteries of the heart leads to the cardiac ailment, myocardial infarction (MI). Myocardial infarction (MI) is also called the heart attack, and it results in the death of heart muscle cells due to the lacking in the supply of oxygen and other nutrients. The early and accurate detection of MI using the 12-lead electrocardiogram (ECG) is helpful in the clinical standard for saving the lives of the patients suffering from this pathology. This paper proposes improved accuracy through skewness based feature extracted using Fourier-Bessel (FB) series expansion based empirical wavelet transform (EWT) with fixed order ranges is introduced for the time-scale decomposition of 12-lead ECG signals to give the multiscale analysis of multi-lead ECG beat. For each lead ECG signal, nine subband signals are evaluated using FBSE-EWT. The statistical features such as the skewness and the entropy are evaluated from the subband signals of each ECG lead. The experimental results demonstrate that FBSE-EWT based skewness features has the mean accuracy, the mean sensitivity and the mean specificity values of 96.58%, 94.71%, and 93.83% ,respectively for the detection of MI using 11-layered proposed CNN architecture. We also achieved an average accuracy of 93.53% and 95.22% using ECG beats with noise and without noise removal respectively

KEYWORDS: Electrocardiogram, Fourier Bessel Series Expansion, Emperical Wavelet Transform, Skewness , Myocardial Infraction

I. INTRODUCTION

In recent years, various techniques have been applied for the automated detection of MI using 12-lead ECG signals[5,6,7,8,9,28] . They have used the coefficients of ST-segments of 12-lead ECG as features for the detection of MI[4]. The accurate detection of ECG on-set points along each lead is the prerequisite for the time-domain feature extraction approaches for MI detection. The shortcomings of wavelet-based approaches for the detection of MI are the requirement of the scaling and wavelet functions as priors for the timescale decomposition of 12-lead ECG, and the selection of the number of decomposition levels. This paper explores the Fourier-Bessel series expansion based EWT (FBSE-EWT)[2] for time-scale analysis of 12-lead ECG, and the extraction of various features. In comparison to conventional EWT, the subband signals extracted using FBSE-EWT method match more firmly to actual narrow-band signal components . Due to the compact spectral representation of signals in the FBSE domain with better resolution, the FBSE-EWT method is very effective to estimate closely spaced frequency components in the analyzed signals. These salient characteristics inspired us to decompose the analyzed 12-lead ECG signals using the FBSE-EWT method, and thereby, extracted features from the sub-band signals. Skewness is asymmetry in a statistical distribution, in which the curve appears distorted or skewed either to the left or to the right. Skewness can be quantified to define the extent to which a distribution differs from a normal distribution. It should be noted that in comparison to conventional EWT, the sub-band signals extracted using FBSE-EWT method match more firmly to actual narrow-band signal components. The repeated convolutional and pooling layers in CNN provides a better representation of ECG feature vector and, thus giving a higher performance for the detection of heart pathology.

II. SYSTEM DESIGN

In this section, the proposed approach for the detection of MI is presented. The approach mainly comprises of two sub-blocks such as, the diagnostic feature extraction from 12-lead ECG data matrix, and detection of MI using CNN. The diagnostic feature extraction process as shown in Fig. 1 consists of the 12-lead ECG data collection, filtering and segmentation of 12-lead ECG data matrix, FBSE-EWT based time-scale decomposition of 12-lead ECG matrix, and evaluation of skewness and kurtosis statistical features.

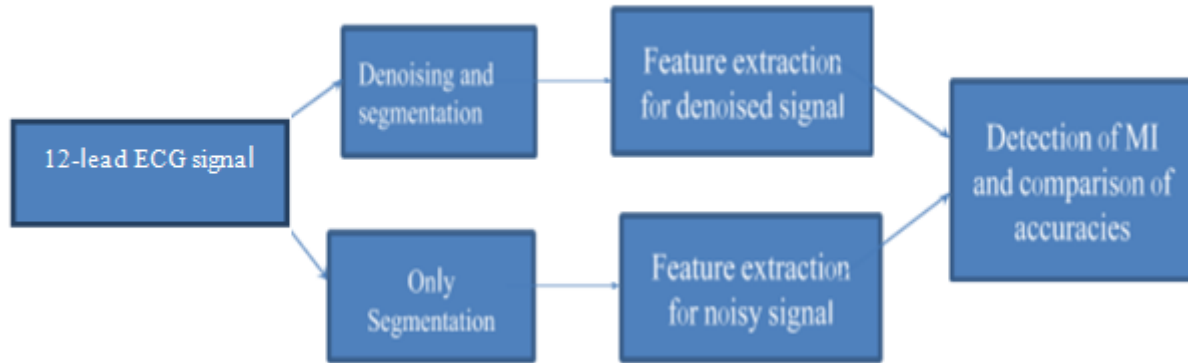


Fig 1. Flow Model of the proposed architecture for detection of MI.

III. METHODOLOGY

We have used the 12-lead ECG data matrix for healthy control (HC) and MI cases from Physikalisch Technische Bundesanstalt (PTB)[15] diagnostic ECG database . This database comprises of 549 records of 15- lead ECG data, out of that the leads such as I, II, III, aVR, aVL, aVF, V1-V6 are 12-lead ECG signals, and the remaining three leads (Vx, Vy and Vz) are vector cardiogram (VCG) signals. In this database, the sampling rate of each lead ECG signal is 1000 Hz, and the amplitude range is 16.384 mV with 16-bit resolution. In this study, we have taken 100, and 74 numbers of 12-lead ECG recordings from 100 MI and 52 HC subjects, and each 12-lead ECG recording has a duration of 24 hours.

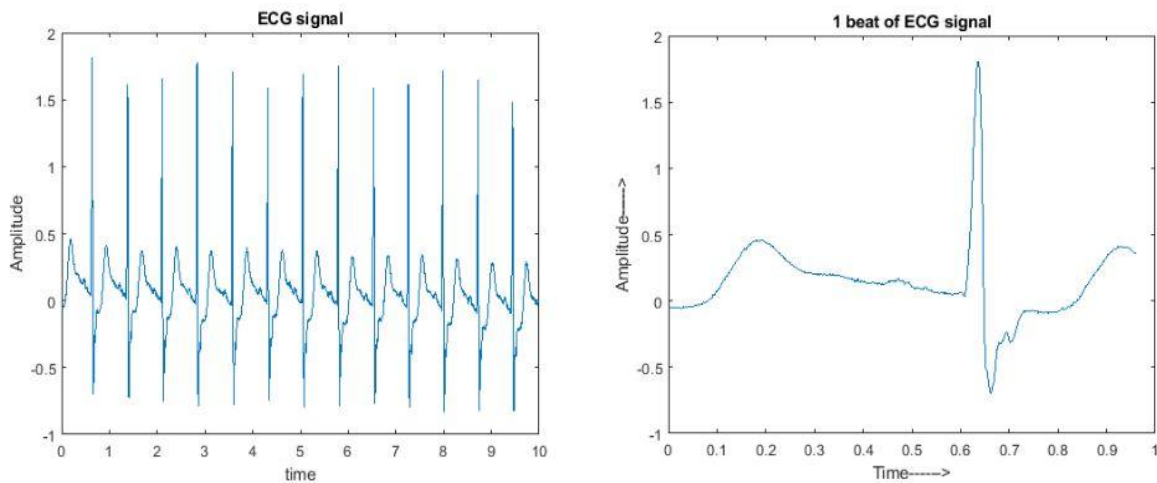


Fig 2: lead V9 ECG signal from PTB database and a beat segmented plot of it.

The filtering process is applied to each 12-lead ECG data recording for HC and MI cases. The baseline wandering noise is filtered out using a Butterworth second order high-pass filter with the cutoff frequency as 0.5 Hz. The segmentation of the filtered 12-lead ECG data matrix is done using a rectangular window of size 4000 X 12. From each 24 hours recording of 12-lead ECG data, the non-overlapping frames are extracted. To capture all three types of correlations or similarities such as intra-beat, inter-beat and inter-lead in 12-lead ECG, we have used frame based segmentation technique.

The underlying concept of FBSE-EWT can be discussed using the following steps as[29]:

1. The FBSE method is employed for obtaining spectral representation of the analyzed signal in the frequency range $[0, \pi]$. The zero-order Bessel functions are used for the series expansion of the analyzed 12-lead ECG signal.

$$P_k^m = \frac{2}{K^2(J_1(\zeta_k))^2} \sum_{n=0}^{K-1} nx^m(n) J_0\left(\frac{\zeta_k n}{K}\right) \dots 1$$

2. The scale-space based boundary detection method is used to find the optimal boundary frequencies and to segregate FBSE spectrum into L number of contiguous segments. This requires the determination of L + 1 boundary frequencies.

TABLE I : Scaling ,Wavelet Functions used in EWT

Scaling [29]	$S_i(l) = \begin{cases} 1 & \text{if } l \leq (1-\epsilon)l_i \\ \cos\left(\frac{\pi\mu(\epsilon, l_i)}{2}\right) & \text{if } (1-\epsilon)l_i \leq l \leq (1+\epsilon)l_i \\ 0 & \text{otherwise} \end{cases}$
Wavelet [29]	$W_i(l) = \begin{cases} 1 & \text{if } (1+\epsilon)l_i \leq l \leq (1-\epsilon)l_{i+1} \\ \cos\left(\frac{\pi\mu(\epsilon, l_{i+1})}{2}\right) & \text{if } (1-\epsilon)l_{i+1} \leq l \leq (1+\epsilon)l_{i+1} \\ \sin\left(\frac{\pi\mu(\epsilon, l_i)}{2}\right) & \text{if } (1-\epsilon)l_i \leq l \leq (1+\epsilon)l_i \\ 0 & \text{otherwise} \end{cases}$

3. A set of band-pass filters are constructed in each segment using empirical scaling and wavelet functions. The wavelet based filters are built based on the construction idea of Littlewood-Paley and Meyer’s wavelets[29,31]. In Table I, the mathematical expression of empirical scaling $S_i(l)$ and wavelet functions $W_i(l)$ are presented. The function $\mu(\epsilon, l_i)$ in Table I is expressed as

$$\mu(\epsilon, l_i) = \gamma\left(\frac{(|l|-(1-\epsilon)l_i)}{2\epsilon l_i}\right) \dots 2$$

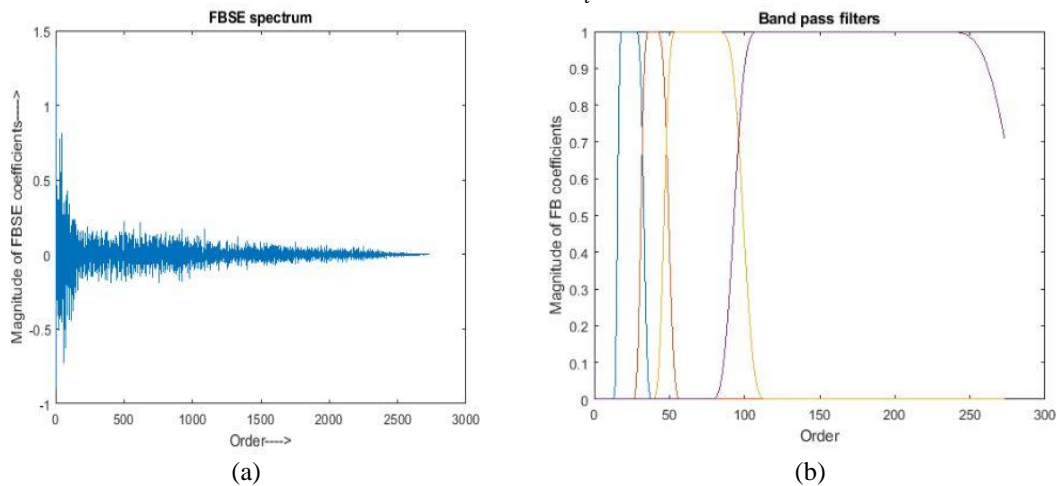


Fig 3 (a) Fourier Bessel Series Expansion spectrum used for calculation of coefficients. (b) A set of pass-band filters used to obtain sub-band signals.

where $y(z)$ is a random function which is given by eq. 3

$$\gamma(y) = \begin{cases} 0, & \text{if } y \leq 0 \\ \text{and } \gamma(y) + \gamma(1-y) = 1 & \forall y \in [0, 1] \dots 3 \\ 1 & \text{if } y \geq 1 \end{cases}$$

4. Approximation coefficients $s_{A_1}(s)$, given in eq. 4, from 12-lead ECG have been computed by evaluating the inner product of the wavelets and scaling function with the ECG signal

$$cD_j^m(s) = \sum_{\tau=1}^N x^m(\tau) \overline{W_i(\tau-s)} \dots 4$$

5. The skewness (SK) and kurtosis(KR) feature for the tth subband signal of mth ECG lead is given by eq. 5,6.

$$SK_t^m = \frac{E(x_t^m(n) - \mu_t)^3}{\sigma_t^3} \dots 5$$

$$KR_t^m = \frac{E(x_t^m(n) - \mu_t)^4}{\sigma_t^4} \dots 6$$

where μ_t and σ_t are called as the average and the standard deviation values for tth subband signal, and E is the expectation operator.

A standard back-propagation with a batch size of 10 is executed in this work. The regularization, momentum, and learning rate parameters are set to 0.2, 3×10^{-4} , and 0.7 respectively. These parameters are tuned accordingly to obtain optimum performance. In this work, we ran a total of 60 epochs of training and testing rounds. At the end of every epoch, our proposed algorithm validates the CNN[18] model. Out of the 9/10 training ECG beats, we used 7/10 to validate our proposed algorithm.

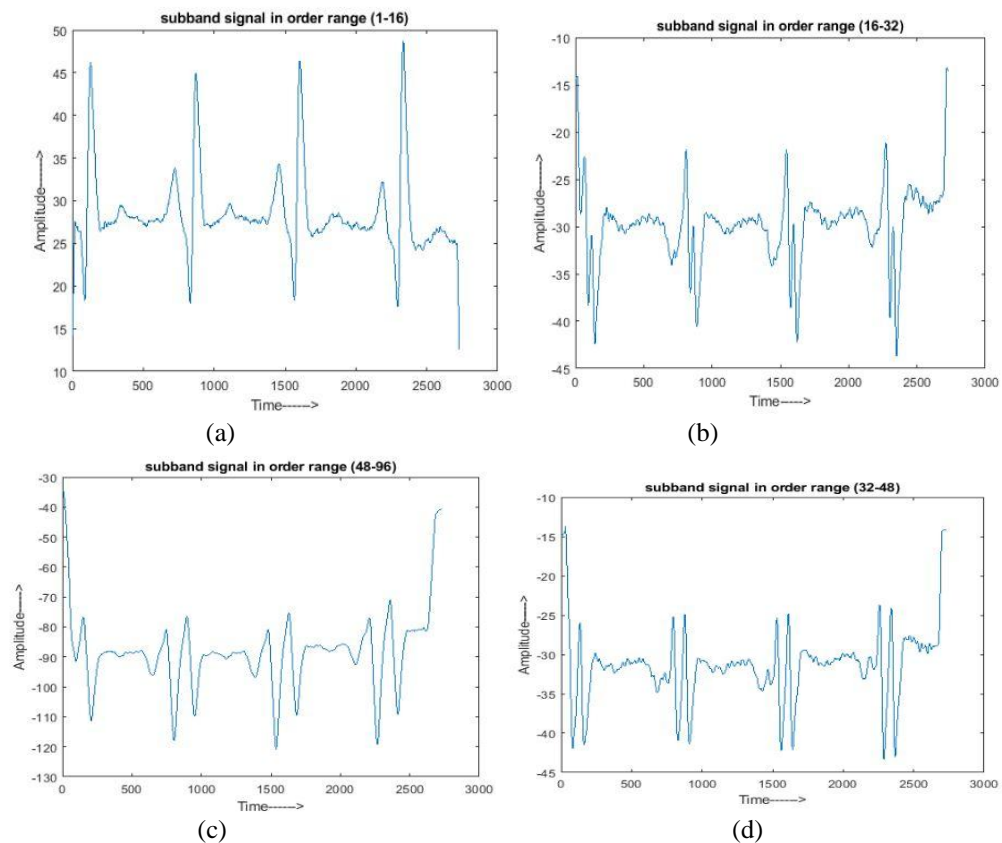


Fig4.(a-d) 4 sub-band signals evaluated by FBSE-EWT based time-scaled decomposition of lead V9 ECG

We have employed a 10-fold cross-validation strategy in this work. We separated our total ECG beats almost equally into 10 segments. 9/10 ECG beats are used in the training of CNN while the remainder (1/10) of the ECG beats are used to validate the performance of our proposed system. This approach is iterated 10 times by shifting the test data. Finally, the performances recorded in all 10 iterations are averaged and considered as the overall performance of our proposed system.

TABLE II: The Details Of CNN Structure

Layer	Layer type	No. of neurons	Kernel size	Stride
0-1	Convolution	550x3	10x2	1
1-2	Max-pooling	275x3	2	2
2-3	Convolution	252x10	10x10	1
3-4	Max-pooling	126x10	2	2
4-5	Convolution	116x10	10x10	1
5-6	Max-pooling	58x10	2	2
6-7	Convolution	50x10	10x10	1
7-8	Max-pooling	25x10	2	2
8-9	Fully-connected	30	-	-
9-10	Fully-connected	10	-	-
10-11	Fully-connected	2	-	-

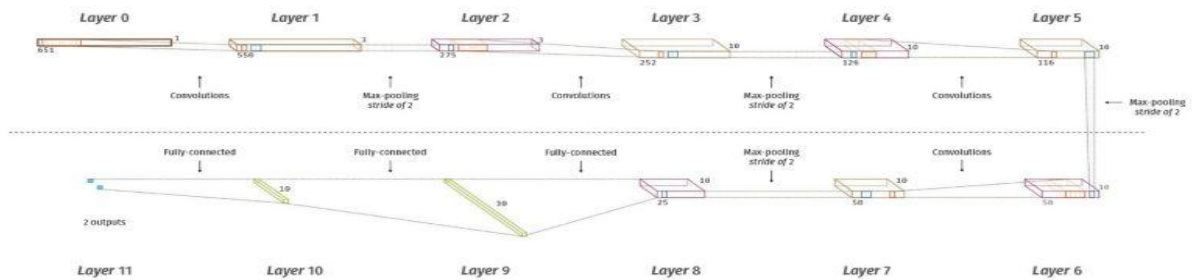


Fig.5: The design of CNN layers used^[6]

IV. EXPERIMENTAL RESULTS

TABLE III: Confusion Matrix of ECG Beats With Noise Across 10-Folds

		Predicted					
		Normal	MI	ACC(%)	PPV(%)	SEN(%)	SPEC(%)
Original	Normal	9750	674	93.53	79.48	92.83	93.71
	MI	2521	37,661	93.49	98.03	93.71	92.83

TABLE IV: Confusion Matrix of ECG Beats Without Noise Across 10-Folds

		Predicted					
		Normal	MI	ACC(%)	PPV(%)	SEN(%)	SPEC(%)
Original	Normal	9970	454	95.63	84.56	94.83	95.71
	MI	1800	38,382	95.53	98.43	95.71	94.83

The confusion matrix for ECG beats with noise and without noise are presented in Tables III and IV respectively. It can be observed from Table III that, out of 10,424 normal ECG beats, approximately 6.46% of the ECG beats are wrongly classified as MI. Likewise, for MI, a total of 6.20% of ECG beats are wrongly classified as normal ECG beats. Similarly, in Table IV, 95.53% of ECG beats are correctly classified as normal ECG beats and 4.35% are

wrongly classified as normal ECG beats. Furthermore, the PPV values for each class (normal and MI) are recorded in Tables III and IV. In Table III, the PPV in the normal class is 79.49% whereas the PPV in the MI class is 98.03%. This shows that the probability of correctly detecting the MI ECG signals from the ECG signals is higher as compared to the correct detection of normal ECG signals. Similarly, in Table IV, the PPV in the normal and MI classes are 84.56% and 98.43% respectively. The performance rate of both noisy and noiseless ECG beats using skewness and kurtosis feature vector is summarized in Table V and VI. Through these it is observed that mean accuracy is more for noiseless ECG beats, even if it is skewness or kurtosis feature vector. The average of noisy and noiseless values are taken as results for Table VII.

TABLE V: The Results for the Classification of Normal and MI Classes Across 10-Folds using **Skewness FV**

SignalType	TP	TN	FP	FN	ACC(%)	PPV(%)	SEN(%)	SPEC(%)
Noisy	37,650	9795	750	2520	93.53	98.40	93.71	92.83
Noiseless	38,360	9930	614	1815	97.63	98.43	95.71	94.83

TABLE VI: The Results for the Classification of Normal and MI Classes Across 10-Folds using **Kurtosis FV**

SignalType	TP	TN	FP	FN	ACC(%)	PPV(%)	SEN(%)	SPEC(%)
Noisy	41,889	5556	750	2520	88.29	98.40	88.93	91.65
Noiseless	45696	2594	614	1815	94.63	98.43	92.71	93.65

It is also evident from Table VII that the performance of CNN classifier using skewness features is higher than the kurtosis for each lead ECG. Moreover, it is also observed that the accuracy, sensitivity and specificity values of kurtosis features are less than 95% using CNN classifier. The kurtosis features fail to capture the pathological variation in the subband signals of each lead ECG and due to this reason these features have less performance for MI detection using CNN classifier. Moreover skewness features calculated using FBSE-EWT decomposition provide better similarity to original signal which is why it is correctly detects the anomaly in ECG signal.

TABLE VII: Performance of CNN Classifier using FV'S from 12-lead ECG.

Measures	Skewness FV	Kurtosis FV
Accuracy(%)	96.58%	91.46%
Sensitivity(%)	94.71%	90.82%
Specificity(%)	93.83%	92.65%

V. CONCLUSION

The early diagnosis of MI can save life and can help to provide timely treatment. Thus, it is necessary to go for annual health checkups. The ECG is the primary tool to diagnose the electrical activity of the heart. Any abnormalities present in the heart activity is reflected in the ECG signals. However, it is challenging and time-consuming to visually assess the ECG signals. Therefore, implementing a CAD system in clinical settings will ensure an objective and fast diagnosis of MI. In this work, we proposed a method to automatically diagnose MI using 11-layer deep CNN. We have used two different datasets to evaluate the effectiveness of our proposed method. We have achieved an average accuracy, sensitivity, and specificity of 93.53%, 93.71%, and 92.83% respectively for ECG beats with noise. Our proposed system attained high-performance results even though there are noises present in the ECG beats. This suggests that our system can recognize the class of the ECG signals even with the presence of noise in the signal. Also, we obtained an average accuracy, sensitivity, and specificity of 95.22%, 95.49%, and 94.19% for ECG beats without noise. We also obtained average, sensitivity, and specificity of 96.58%, 94.71%, 93.83% for skewness feature vector. This shows that the

overall performance of our proposed system is good enough and hence, can be introduced in clinical settings. Our proposed system can assist doctors in their diagnosis.

REFERENCES

- [1] Rajesh Kumar Tripathy, Abhijit Bhattacharyya, and Ram Bilas Pachori A Novel Approach for Detection of Myocardial Infarction from ECG Signals of Multiple Electrodes IEEE Sensors Journal · January 2019
- [2] Abhijit Bhattacharyya , Lokesh Singh, Ram Bilas Pachori “Fourier–Bessel series expansion based empirical wavelet transform for analysis of non-stationary signals” Elsevier 2018
- [3] Rajesh Kumar Tripathy, Abhijit Bhattacharyya, and Ram Bilas Pachori “Localization of Myocardial Infarction from Multi-Lead ECG Signals using Multiscale Analysis and Convolutional Neural Network” IEEE Sensors Journal · January 2019
- [4] J. J. Bax, H. Baumgartner, C. Ceconi, V. Dean, R. Fagard, C. FunckBrentano, D. Hasdai, A. Hoes, P. Kirchhof, J. Knuuti et al., “Third universal definition of myocardial infarction,” *Journal of the American College of Cardiology*, vol. 60, no. 16, pp. 1581–1598, 2012
- [5] S. Ansari, N. Farzaneh, M. Duda, K. Horan, H. B. Andersson, Z. D. Goldberger, B. K. Nallamothu, and K. Najarian, “A review of automated methods for detection of myocardial ischemia and infarction using electrocardiogram and electronic health records,” *IEEE reviews in biomedical engineering*, vol. 10, pp. 264–298, 2017.
- [6] U. R. Acharya, H. Fujita, V. K. Sudarshan, S. L. Oh, M. Adam, J. E. Koh, J. H. Tan, D. N. Ghista, R. J. Martis, C. K. Chua et al., “Automated detection and localization of myocardial infarction using electrocardiogram: a comparative study of different leads,” *Knowledge-Based Systems*, vol. 99, pp. 146–156, 2016
- [7] M. Arif, I. A. Malagore, and F. A. Afsar, “Detection and localization of myocardial infarction using k-nearest neighbor classifier,” *Journal of medical systems*, vol. 36, no. 1, pp. 279–289, 2012
- [8] A. K. Dohare, V. Kumar, and R. Kumar, “Detection of myocardial infarction in 12 lead ecg using support vector machine,” *Applied Soft Computing*, vol. 64, pp. 138– 147, 2018
- [9] R. Tripathy and S. Dandapat, “Detection of cardiac abnormalities from multilead ecg using multiscale phase alternation features,” *Journal of medical systems*, vol. 40, no. 6, p. 143, 2016.
- [10] L. Sun, Y. Lu, K. Yang, and S. Li, “Ecg analysis using multiple instance learning for myocardial infarction detection,” *IEEE transactions on biomedical engineering*, vol. 59, no. 12, pp. 3348–3356, 2012.
- [11] S. Xu, M. Mak, and C. Cheung, “Towards end-to-end ecg classification with raw signal extraction and deep neural networks.” *IEEE journal of biomedical and health informatics*, 2018.
- [12] L. G. Tereshchenko and M. E. Josephson, “Frequency content and characteristics of ventricular conduction,” *Journal of electrocardiology*, vol. 48, no. 6, pp. 933–937, 2015.
- [13] M. Sharma, R. San Tan, and U. R. Acharya, “A novel automated diagnostic system for classification of myocardial infarction ecg signals using an optimal biorthogonal filter bank,” *Computers in biology and medicine*, 2018.
- [14] L. Sharma, R. Tripathy, and S. Dandapat, “Multiscale energy and eigenspace approach to detection and localization of myocardial infarction,” *IEEE transactions on biomedical engineering*, vol. 62, no. 7, pp. 1827–1837, 2015
- [15] M. Oeff, H. Koch, R. Boussejot, and D. Kreiseler, “The ptb diagnostic ecg database,” *National Metrology Institute of Germany*, 2012.
- [16] L. Goldberger, L. A. Amaral, L. Glass, J. M. Hausdorff, P. C. Ivanov, R. G. Mark, J. E. Mietus, G. B. Moody, C.-K. Peng, and H. E. Stanley, “Physiobank, physiotoolkit, and physionet: components of a new research resource for complex physiologic signals,” *Circulation*, vol. 101, no. 23, pp. e215–e220, 2000.
- [17] I. Goodfellow, Y. Bengio, A. Courville, *Deep Learning*, MIT Press, 2016 <http://www.deeplearningbook.org>.
- [18] M. Arif , I.A. Malagore , F.A. Afsar , Detection and localization of myocardial infarction using K-nearest neighbor classifier, *J. Med. Syst.* 36 (2012) 279–289 .
- [19] H. Greenspan, R.M. Summers, B. van Ginneken, *Deep learning in medical imaging: overview and future promise of an exciting new technique*, *IEEE Trans. Med. Imaging* 35 (5) (2016) 1153–1159.
- [20] M.J.J.P. van. Grinsven, B. van Grinneken, C.B. Hoyng, T. Theelen, C.I. Sánchez, *Fast convolutional neural network training using selective data sampling: application to hemorrhage detection in color fundus images*, *IEEE Trans. Med. Imaging* 35 (5) (2016) 1273–1284.
- [21] V. Gulshan, L. Peng, M. Coram, M.C. Stumpe, D. Wu, A. Narayanaswamy, S. Venugopalan, K. Widner, T. Madams, J. Cuadros, R. Kim, R. Raman, P.C. Nelson, J.L. Mega, D.R. Webster, *Development and validation of a deep learning algorithm for detection of diabetic retinopathy in retinal fundus photographs*, *JAMA* 16 (22) (2016) 2402–2410.



- [22] N. Hatipoglu, G. Bilgin, Cell segmentation in histopathological images with deep learning algorithms by utilizing spatial relationships, *Med. Biol. Eng. Comput.* (2017) 1–20, doi:10.1007/s11517-017-1630-1.
- [23] He.K. Zhang, X. Ren, S. Sun, Delving deep into rectifiers: surpassing human-level performance on image net classification, 1026–1034, 2015.
- [24] E.S. Jayachandran, K.P. Joseph, U.R. Acharya, Analysis of myocardial infarction using discrete wavelet transform, *J. Med. Syst.* 34 (2010) 985–992.
- [25] M. Kallenberg, K. Petersen, M. Nielsen, Y.A. Ng, P.F. Diao, C. Igel, C.M. Vachon, K. Holland, R.R. Winkel, N. Karssemeijer, M. Lillholm, Unsupervised deep learning applied to breast density segmentation and mammographic risk scoring, *IEEE Trans. Med. Imaging* 35 (5) (2016) 1322–1331.
- [26] A. Krizhevsky, I. Sutskever, G.E. Hinton, ImageNet classification with deep convolutional neural networks, *Neural Information Processing Systems Conference*, 25, 2012.
- [27] D.K. Kulick, J.W. Marks, C.P. Davis, Heart Attack (Myocardial Infarction), 2015. Retrieved from http://www.medicinenet.com/heart_attack/article.htm.
- [28] T. Lahiri, U. Kumar, H. Mishra, S. Sarkar, A.D. Roy, Analysis of ECG signal by chaos principle to help automatic diagnosis of myocardial infarction, *J. Scient. Industr. Res.* 68 (2009) 866–870.
- [29] J. Gilles, “Empirical wavelet transform,” *IEEE Transactions on Signal Processing*, vol. 61, no. 16, pp. 3999–4010, 2013.
- [30] R. B. Pachori and P. Sircar, “Non-stationary signal analysis: Methods based on Fourier-Bessel representation,” LAP LAMBERT Academic Publishing, Germany, 2010.
- [31] I. Daubechies, Ten lectures on wavelets, CBMS-NSF Regional Conference Series in Applied Mathematics, SIAM, Philadelphia, PA, USA, 1992, vol. 61.